ACS Catalysis

Research Article

pubs.acs.org/acscatalysis

Effects of Thiol Modifiers on the Kinetics of Furfural Hydrogenation over Pd Catalysts

Simon H. Pang,[†] Carolyn A. Schoenbaum,[†] Daniel K. Schwartz, and J. Will Medlin*

Department of Chemical and Biological Engineering, University of Colorado Boulder, Boulder, Colorado 80309, United States

Supporting Information

ABSTRACT: Thiolate self-assembled monolayers (SAMs) were used to block specific active sites on Pd/Al_2O_3 during the hydrogenation of furfural to elucidate site requirements for each process involved in this complex reaction network. Reactions were performed on uncoated, 1-octadecanethiol (C18) coated, and benzene-1,2-dithiol (BDT) coated catalysts. Selectivity among key reaction pathways was sensitive to the SAM modifier, with increasing sulfur density strongly suppressing furfural decarbonylation, less strongly suppressing furfural hydrogenation, and minimally affecting furfuryl alcohol hydrodeoxygenation to methylfuran. Diffuse reflectance infrared Fourier transform spectroscopy with CO was used to characterize site availability on the catalysts. The presence of a C18 modifier restricted the availability of Pd terrace sites, while accessibility to Pd edges and steps was practically unaffected with respect to the uncoated catalyst. The BDT modifier further restricted terrace accessibility but additionally restricted adsorption at particle edges and steps. Comparison between reaction rates and site availability suggested that decarbonylation occurred primarily on terrace sites, while hydrodeoxygenation occurred on particle steps and edges. Aldehyde hydrogenation, and its reverse process of alcohol dehydrogenation, was found to occur on both terrace or edge sites, with the dominant pathway dependent on surface coverage as determined by reaction conditions. The results of a detailed kinetic study indicate that in addition to changing the availability of specific sites, thiol monolayers can strongly affect reaction energetics and decrease the coverage of strongly adsorbed furfural-derived intermediates under reaction conditions. Ambient pressure X-ray photoelectron spectroscopy experiments indicated that the metal−sulfur bonds were not changed appreciably under reaction conditions. The results of this work show that HDO is not appreciably affected even with drastic decreases in the density of available sites as measured by CO adsorption, providing opportunities to design isolated catalyst sites for selective reaction.

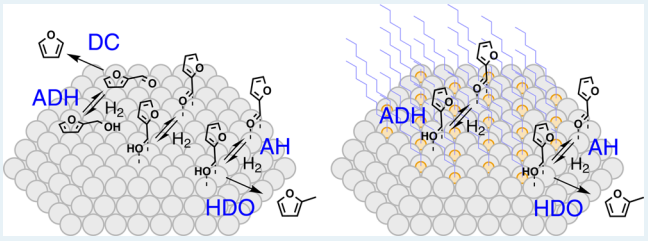

KEYWORDS: *heterogeneous catalysis, self-assembled monolayers, alkanethiol, furfural, palladium*

INTRODUCTION

Self-assembled monolayers (SAM) of organic thiolates have been used as surface modifiers to influence the reactivity of heterogeneous catalysts.[1] On Pd, thiols undergo S−H bond dissociation, and the resulting surface thiolates assemble into well-ordered structures on both flat, polycrystalline surfaces and supported catalysts.[2−4] SAMs are attractive for use as surface modifiers because they form ordered overlayers of predictable density according to the functionality of the tail group utilized. SAMs have recently attracted attention because their presence on catalyst surfaces has been shown to dramatically influence the reaction selectivity for molecules with multiple functional groups.[4−6] In some cases, this reaction selectivity change has been ascribed to the presence of the SAM preventing a particular, often multicoordinated, adsorption conformation of the reactant. For example, Wu et al. recently demonstrated that an amine capping layer on Pt_3Co nanocatalysts prevented α,β-unsaturated aldehydes from lying flat on the surface, inhibiting direct contact of the C═C bonds with the catalyst and resulting in a dramatic improvement to the corresponding alcohol.[7] Unsupported thiol-coated Pd nanoparticles have also been used for Heck[8,9] and Suzuki[10−12] carbon−carbon cross-coupling reactions as well as selective isomerization of allyl alcohol[13] and hydrogenation of allylamine.[14]

There is strong evidence suggesting that specific types of sites or groups of sites may be required in order for a particular pathway to occur.[15] Traditionally, the relationship between reactivity and site requirement has been probed using particle size.[16] Smaller particles are expected to have a higher fraction of particle edge sites than larger particles. Therefore, if the rate of formation of a particular product is found to increase with decreasing particle size, it is likely that this reaction occurs preferentially at edge sites. Conversely, if the opposite trend is observed, the reaction likely requires a site or group of sites located on the particle terraces. While particle size experiments provide information about reaction pathways, it can be difficult to synthesize and characterize particles with specific and systematic size variation; small discrepancies in synthesis conditions can result in significant changes in resulting particle morphology.[17] An alternative approach for discerning the

Received: May 2, 2014
Revised: July 31, 2014

   dx.doi.org/10.1021/cs500598y | ACS Catal. 2014, 4, 3123−3131

Scheme 1. Furfural Hydrogenation Pathways over Pd

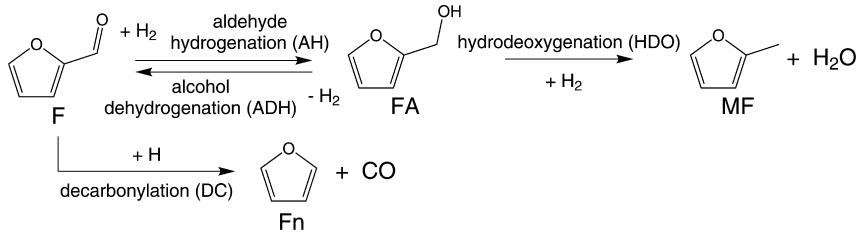

locations of individual reaction steps is to selectively block specific types of sites, e.g. with SAMs. This approach is particularly useful for complex reaction systems in which a number of simultaneous processes may be occurring. By understanding the types of surface environments required for particular reaction pathways, we can improve our ability to design more selective catalysts.

Furfural is an important probe molecule for understanding key reactions of biomass derivatives for synthesis of chemicals and fuels.[18,19] On Pd catalysts, furfural (F) binds strongly through its aromatic ring, resulting primarily in decarbonylation (DC) to produce furan (Fn). Steps such as aldehyde hydrogenation (AH) and hydrodeoxygenation (HDO), which are desirable for conversion of aldehydes to fuels such as methylfuran (MF), do not occur readily. Additionally, the aldehyde hydrogenation pathway is reversible, and furfuryl alcohol (FA) can undergo alcohol dehydrogenation (ADH) to form furfural on the surface. These reaction processes and the adsorption of furfural have been studied in detail on the Pd(111) surface with density-functional theory[20] and temperature-programmed desorption.[21] Scheme 1 depicts the reaction pathways described here.

We recently demonstrated that the surface density of the SAM can be controlled to systematically reduce the number of contiguous sites on particle terraces, while leaving accessibility to edges and steps largely unaffected, resulting in improved selectivity toward hydrogenation and hydrodeoxygenation products during furfural hydrogenation.[22] While desirable reaction pathways were generally found to be associated with reactions at particle edge sites, the individual reaction processes were not treated independently to obtain mechanistic information about the formation of intermediate products. More generally, there have been few detailed kinetic studies of the hydrogenation of furfural on late transition metal catalysts. A recent density functional theory study has illustrated some of the reaction pathways on Pd(111) in vacuum,[20] but these calculations were performed at low adsorbate coverage. Thus, corroboration with experimental kinetic measurements can provide key additional insights at the elementary step level for these complex reaction networks.

Here we report a systematic kinetic analysis of the hydrogenation pathways of furfural over Pd catalysts. Our aim was to understand the effects on reaction mechanism of modification by either 1-octadecanethiol (C18), which forms a $(\sqrt{3} \times \sqrt{3})$R30 structure on the Pd(111) surface (0.33 fractional coverage of sulfur),[2] or benzene-1,2-ditihiol (BDT), which has been shown on Pt(111) to form a $p(2 \times 2)$ structure in the thiol,[23] to investigate the influence of a high density of metal−sulfur bonds (up to 0.50 fractional coverage of sulfur). Selection of these two thiol modifiers is based on the hypothesis that ensemble of adjacent surface sites can be further restricted by an increased number of metal-modifier attachments, which will have a large effect on furfural hydrogenation selectivity.

METHODS AND MATERIALS

Catalyst Preparation. Thiol-coated catalysts were prepared by immersing 5 wt % Pd/Al_2O_3 (SigmaAldrich Lot no. MKBH9857V) in a 5 mM ethanolic solution of 1-octadecanethiol (C18, 98%, SigmaAldrich) or benzene-1,2-dithiol (BDT, 96%, SigmaAldrich) for at least 12 h. The supernatant was decanted, and the catalysts were rinsed in ethanol to remove any physisorbed thiol. The catalysts were allowed to settle, the rinsing solution was decanted, and the catalysts were dried in air overnight before use. Sulfur content of supported catalysts was analyzed using inductively coupled plasma optical emission spectrometry (ICP-OES).

Infrared Spectroscopy. FTIR analysis was performed using a Thermo Scientific Nicolet 6700 FT-IR with a closed cell attachment (Harrick) for diffuse reflectance infrared Fourier transform spectroscopy (DRIFTS). To determine information about the structure and integrity of monolayer formation, spectra were collected in the hydrocarbon stretching region for the C18- and BDT-modified catalysts. These spectra can be found in Figure S1. For the C18 catalyst, the position of the asymmetric methylene stretch at ∼2922 cm^{-1} indicated a relatively well-ordered monolayer with few gauche defects; this stretch appears at 2918 cm^{-1} in crystalline docosanethiol.[24] For the BDT catalyst, the absorption feature at ∼3050 cm^{-1} was attributed to the C−H ring stretch of the phenyl moiety. For CO DRIFT experiments, catalyst samples were first exposed to reaction conditions for 2 h at mole fractions y_{H2} = 0.250 and $y_{furfural}$ = 0.010 and a reaction temperature of 190 °C. Samples were then placed in a gastight cell that was evacuated to achieve a baseline pressure of 0.15 Torr. CO was then introduced into the cell to a pressure of 2.00 Torr at which point spectra were collected. 100 scans at 4 cm^{-1} resolution were used for each spectrum.

CO Chemisorption. Active metal surface area measurement was performed on a Micromeritics ChemiSorb 2720. Approximately 100 mg of as-purchased Pd catalyst was reduced in 20 sccm H_2 at 200 °C for 3 h and then purged in 20 sccm Ar at 200 °C for 20 h without exposure to air. CO pulse chemisorption was performed at 50 °C using 1 mL injections of 20% CO (balance Ar). Injections were performed until there was no change in the amount of CO detected, indicating that none was adsorbing. Using this technique, the active metal surface area was calculated to be approximately 3.8 m^2/g catalyst (17% dispersion) with a CO uptake of approximately 7.9×10^{-5} μmol CO/g catalyst, corresponding to an average Pd particle size of 8.3 nm.

X-ray Photoelectron Spectroscopy. The types of sulfur present on the catalysts were characterized using (near) ambient pressure X-ray photoelectron spectroscopy (AP-

dx.doi.org/10.1021/cs500598y | ACS Catal. 2014, 4, 3123−3131

XPS). Thin films of Pd were prepared by thermal evaporation onto a Si wafer using a CVC 3-boat thermal evaporator. A bonding layer of 1.5 nm Cr was used, onto which 200 nm of Pd was deposited at a rate of 0.7 nm/s. Thiol coatings were prepared in a similar manner to the supported catalyst, using a 1 mM ethanolic solution of thiol. After rinsing in ethanol, the thin films were removed from the solution, and excess solution was wicked away and finally dried in air.

AP-XPS experiments were performed at Brookhaven National Laboratory at the National Synchrotron Light Source, beamline X1A1.[25] In brief, a differentially pumped hemispherical analyzer (Specs Phoibos 150 NAP) was positioned at 70° with respect to the incident X-ray beam and 20° to the surface normal. The sample was positioned 0.5 mm from the aperture to ensure that the local surface pressure was not affected by differential pumping. The temperature was measured with a type K thermocouple spot-welded to a Ta backplate located between the heater and crystal. All spectra intensities were normalized with respect to the NSLS ring current. Pd 3d and S 2p spectra were collected at a photon energy of 562 eV. In situ spectra were taken by exposing the sample to 0.1 Torr furfural and 0.5 Torr H_2, while the sample was heated to 190 °C. Postreaction spectra were taken under vacuum after exposure of the thin film to reaction conditions for over 2 h.

XPS analysis and peak deconvolution were performed in OriginLab 9.0. Baseline subtractions were performed using the Shirley method.[26] Peaks were fit using a pseudo-Voigt function composed of the sum of 70% Gaussian and 30% Lorentzian. The S $2p_{3/2}/2p_{1/2}$ peak area ratio was fixed at 2:1, and the peaks were fit with a doublet separation of 1.19 ± 0.02 eV. Spectra for BDT- and C18-coated Pd thin films were obtained on separate trips to BNL; in the interim, the system was better optimized, allowing for larger spectra intensities for the C18-coated thin film, and so intensities between the C18 and BDT thin films were not directly comparable. Thus, peaks on the BDT surface were fit with Gaussian and Lorentzian fwhm at 1.63 ± 0.04 eV, and peaks on the C18 surface were fit with fwhm at 1.38 ± 0.03 eV. Spectra obtained under vacuum, both before and after reaction, with fits and a summary of the peak area fractions can be found in Figure S2 and Table S1.

Catalytic Reactions. Hydrogenation reactions were performed in a tubular packed bed flow reactor at atmospheric pressure and constant total gas flow rate. Helium was bubbled through furfural or furfuryl alcohol which was immersed in a water bath to control the temperature. The saturated helium was mixed with H_2 and diluent He before being passed through the catalyst bed. All gases were obtained at ultrahigh purity from Airgas. The temperature of the water bath was varied to change the gas phase concentration of furfural/furfuryl alcohol, and the flow rates of H_2 and diluent He were varied to change the concentration of H_2. The amount of catalyst used in each experiment was varied systematically to achieve a conversion of <10% in all cases. All data are reported after at least 2 h on stream.

The gas mixture passed through the catalyst bed, and the reactor effluent was analyzed using an Agilent Technologies 7890A gas chromatograph with a 30 m × 0.320 mm Agilent HP-5 (5% phenyl)-methylpolysiloxane capillary column and flame ionization detector (split ratio = 25:1, column flow rate = 2 mL min^{-1}, oven temperature = 40 °C). Turnover frequencies used to perform reaction order and activation energy analyses were calculated by dividing the product flow rates by the number of surface sites on the unmodified catalyst, based on measurement of active metal surface area from CO chemisorption and mass of catalyst used. Turnover frequencies for AH and ADH processes were calculated based on the reactor effluent; the reversibility of the reaction was not taken into account. Thus, reported TOFs for these processes represent lower bounds for the actual TOFs.

Apparent activation energy studies were performed using the mole fractions y_{H2} = 0.400 and $y_{furfural}$ = 0.010 or $y_{furfuryl\ alcohol}$ = 0.001 at reactor temperatures ranging from 160 to 190 °C. Apparent reaction order studies were performed at a reactor temperature of 190 °C. For reaction orders in furfural and furfuryl alcohol, the hydrogen mole fraction was held constant at y_{H2} = 0.400. For reaction orders in hydrogen, the furfural and furfuryl alcohol mole fractions were held constant at $y_{furfural}$ = 0.010 and $y_{furfuryl\ alcohol}$ = 0.001, respectively. Analysis of these experiments assumed that the rate of each reaction could be expressed in a power law form

$$\text{rate} = k \times {y_F}^{\alpha} \times {y_{H2}}^{\beta}$$

where y_F represents the mole fraction in the gas phase of either furfural or furfuryl alcohol. The activation energies and reaction orders were determined by performing linear regression analysis with inverse variance weighting of the data points. The errors reported are the standard errors in the slopes of the Arrhenius or power law plot. For all catalysts, we ensured that external mass transport was not a limiting factor by varying the weight hourly space velocity.

RESULTS

Uncoated Catalyst Characterization. The uncoated catalyst was characterized using a combination of CO chemisorption and CO DRIFTS. The chemisorption uptake of 75 m^2/g of metal was consistent with an average Pd particle size of 8.3 nm. The CO DRIFT spectrum for the uncoated catalyst after reduction is shown in Figure S3. The catalyst used in this study had features attributable to CO bound in atop (∼2040−2080 cm^{-1}), bridge (∼1980 cm^{-1}) and hollow sites (∼1850−1940 cm^{-1}). Note that the measured average Pd particle size for the catalyst used in these studies was larger than that for catalysts used in our previous work (∼6 nm). This resulted in a significant reduction of CO bound to bridge sites on particle edges and steps for the larger particles used in this study (see Supporting Information for details).

X-ray Photoelectron Spectroscopy. Near ambient-pressure XPS was used to characterize the state of sulfur on the surface both before and during exposure to reaction conditions. Analysis of sulfur species (Figure 1) indicated three types of sulfur on the surface, with $2p_{3/2}$ binding energies of 161.99 ± 0.06, 162.90 ± 0.04, and 163.75 ± 0.04 eV, which have previously been assigned to sulfur bound as thiolate, thiol, and disulfide, respectively.[27,28] All three of these sulfur species were observed under vacuum before reaction, under reaction conditions, and under vacuum after reaction (spectra for catalysts under vacuum both before and after reaction can be found in Figure S2).

The peak associated with weakly adsorbed thiol at 162.90 eV decreased in intensity over the course of the reaction, suggesting that physisorbed thiol precursor molecules were gradually removed. In contrast, the peaks associated with more strongly bound sulfur, thiolate and disulfide, did not change in intensity. Figure S4 demonstrates the evolution of the three

dx.doi.org/10.1021/cs500598y | ACS Catal. 2014, 4, 3123−3131

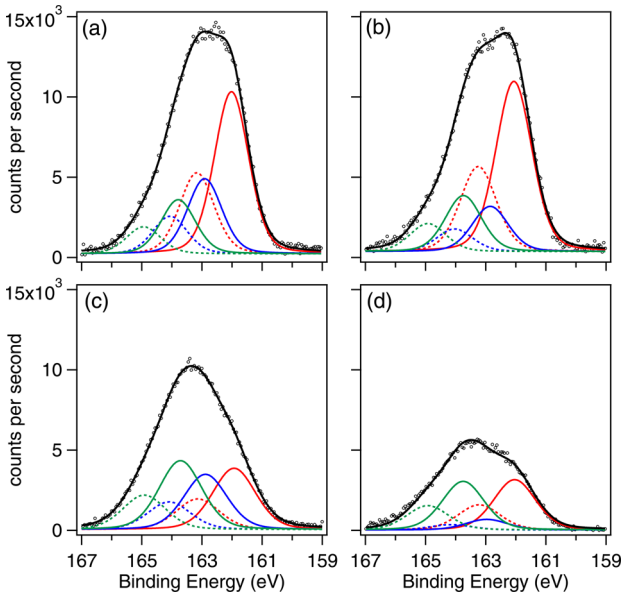

Figure 1. X-ray photoelectron spectra (open circles) in the S 2p region taken in situ under reaction conditions for (a), (b) the C18-coated thin film and (c), (d) the BDT-coated thin film. Spectra (a) and (c) were taken upon introduction of gases and heating to 190 °C. Spectra (b) and (d) were obtained after exposure to reaction conditions for 2 h. S $2p_{3/2}/2p_{1/2}$ doublet separation = 1.19 ± 0.02 eV (solid/dashed colored lines). Intensities between C18 and BDT spectra are not directly comparable (see Methods Section).

peaks for the BDT-coated catalyst over the course of the reaction. This suggests that the decrease in spectra intensity was due to loss of weakly bound sulfur species and that the strong metal−sulfur bonds on the surfaces of the catalysts did not change appreciably over the course of the reaction, despite the presence of hydrogen.

Comparison of sulfur coverage on C18 and BDT catalysts after 2 h under reaction conditions was achieved by normalization based on the Pd signal (Figure S5). The attenuation in electron flux due to the organic layer has been studied previously for electron kinetic energies in the range 500−1500 eV.[29] Under the assumption that the linear relation was still valid at 400 eV (the approximate measured kinetic energy of the detected S 2p electrons) the signal was attenuated to approximately 29% and 78% of the electron flux from the uncoated catalyst for the catalysts with C18 and BDT monolayers, respectively. The S $2p_{3/2}$ signals were normalized against the Pd $3d_{5/2}$ signal, taking into account the inelastic mean free path of the approximately 227 eV electrons in Pd and the signal attenuation due to the organic layer. From in situ XPS data, we calculated that the BDT-coated surface had approximately 50% more sulfur than the C18-coated surface, in agreement with the theoretically expected value of 50% based on the nominal surface structure of the two thiols on single crystal surfaces.

Selectivity over Thiol-Modified Catalysts. Gas-phase hydrogenation of furfural or furfuryl alcohol was conducted in a tubular packed bed flow reactor at 190 °C on 5 wt % Pd/Al_2O_3 that was either left uncoated or was coated with a self-assembled monolayer of 1-octadecanethiol (C18) or benzene-1,2-dithiol (BDT). The Pd surface area of the uncoated catalyst was used for all turnover frequency calculations. Because a large fraction of Pd sites are occupied by thiol modifiers on the coated catalysts, this results in an under-reporting of the "true" turnover frequency, as discussed in more detail below.

Figure 2a reports the turnover frequency obtained at 8 ± 1% conversion of furfural. Using uncoated Pd catalysts, the

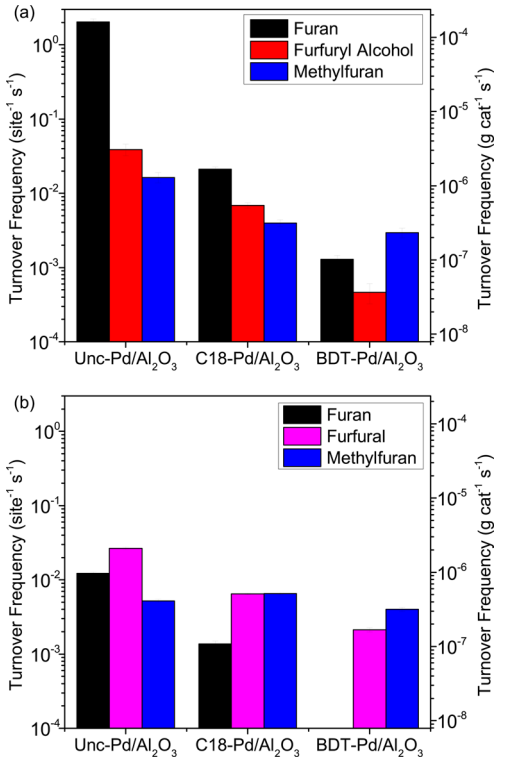

Figure 2. Turnover frequencies for various products from (a) furfural hydrogenation (y_F = 0.010 and y_{H2} = 0.250) and (b) furfuryl alcohol hydrogenation (y_{FA} = 0.001 and y_{H2} = 0.300) over uncoated, C18-coated and BDT-coated 5 wt % Pd/Al_2O_3. Turnover frequencies are reported per surface Pd atom ($site^{-1}$ s^{-1}) where the number of surface atoms was determined from the clean, uncoated catalyst. Selectivity and rate are reported under 10% conversion of reactant fed. Error bars indicate the standard deviation of five repeated measurements of product concentration over the course of an hour.

dominant product was furan (>95% selectivity), and the rate of decarbonylation (DC) was about 2 orders of magnitude greater than those of aldehyde hydrogenation (AH) and hydrodeoxygenation (HDO). C18-coated catalysts exhibited a modest increase in selectivity to the desired AH/HDO products and reached a combined selectivity of about 34%. As shown in Figure 2(a), this selectivity enhancement was achieved through a large decrease in the rate of decarbonylation, and a more modest decrease in the rate of hydrogenation. BDT-coated catalysts, with more sulfur on the surface, continued this trend, reaching a combined AH/HDO selectivity of over 70%. Accordingly, the rate of DC was reduced by 3 orders of magnitude from the uncoated case, whereas the rate of hydrogenation was only reduced by 1 order of magnitude. These selectivity and rate observations may be partially explained by a site-blocking mechanism. The availability of active sites was systematically reduced through the use of C18[2] and BDT[23] SAMs which form monolayers with approximate sulfur coverages of 0.33 and 0.50, respectively. Elemental analysis via ICP-OES demonstrated that after 2 h under reaction conditions there was approximately 66% more sulfur present on the BDT catalysts than the C18 catalysts, in

dx.doi.org/10.1021/cs500598y | ACS Catal. 2014, 4, 3123−3131

agreement with the theoretically expected value and XPS results. The selectivity trends obtained here for the C18-coated catalyst were consistent with those we previously reported, but the quantitative effect of the coating on rates and selectivities was slightly different.[22] Note that the previous results were reported at a different conversion (13%), feed mole fractions (y_{H2} = 0.400 and $y_{furfural}$ = 0.016), and for a more highly dispersed Pd catalyst.

Figure 2b reports the rate obtained at 3 ± 1% conversion of furfuryl alcohol. The mole fraction of furfuryl alcohol was chosen to reflect the amount of furfuryl alcohol produced in the experiments performed from furfural in Figure 2a. Increasing the thiol coverage caused an increase in the selectivity of methylfuran from 12% on the uncoated catalyst to 65% on the BDT-coated catalyst. The combined rates for furfural and furan production were reduced by about a factor of 20 with the BDT modifier. Remarkably, even in the presence of large amounts of sulfur on the surface, the rate of production of methylfuran on the C18-coated catalyst was unaffected and only reduced by a factor of 2 on the BDT-coated catalyst. Thus, while the rate of furfural decarbonylation decreased by between 2 and 3 orders of magnitude for the C18- and BDT-coated catalysts, the rate of furfuryl alcohol hydrodeoxygenation was practically unaffected. This finding indicates that thiolate-modified surfaces can function to catalyze certain reactions without lowering the reaction rate compared to the uncoated surface. As discussed in further detail below, it also suggests that sites optimal for furfuryl alcohol HDO are largely distinct from sites for DC.

CO DRIFTS on Postreaction Catalysts. To directly test the availability of specific adsorption sites on the modified and unmodified catalysts after exposure to reaction conditions, diffuse reflectance Fourier transform infrared spectroscopy (DRIFTS) was performed using carbon monoxide as a probe molecule. Spectra for catalysts before exposure to reaction conditions can be found in Figure S6. In these experiments, peak positions were readily attributed to CO binding in hollow, bridging, and top sites.[30] DRIFT spectra during a saturating exposure of CO on the uncoated, C18, and BDT catalysts are shown in Figure 3.

Previous attempts to elucidate site information on catalysts used CO adsorption before catalysts were exposed to reaction conditions. Since carbonaceous deposits formed during reaction may alter the types of sites available, the experimental results in Figure 3 were collected after reaction to characterize sites available under reaction conditions. With increasing thiol density, the availability of sites on particle terraces (~1895 cm^{-1}) was systematically reduced. Accessibility to particle edges and steps (~2050 cm^{-1}) was essentially unchanged between the uncoated and C18 catalyst but was significantly reduced on the BDT catalyst.

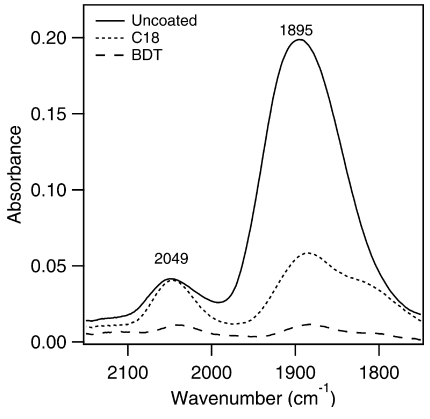

Figure 3. CO stretching region for uncoated, C18- and BDT-modified 5 wt % Pd/Al_2O_3 after exposure to reaction conditions for 2 h.

By comparing the available sites on these catalysts with the differential rates of each reaction, we elucidated the types of sites required for each particular reaction pathway shown in Scheme 1. The rates of DC and AH from reaction of furfural and the rates ADH and HDO from the reaction of furfuryl alcohol are shown together in Figure 4.

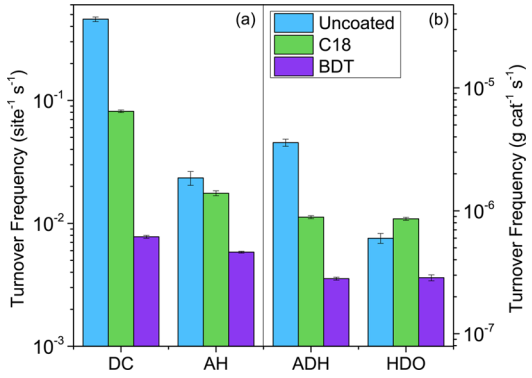

Figure 4. Differential rates of (a) decarbonylation and aldehyde hydrogenation of furfural and (b) alcohol dehydrogenation and hydrodeoxygenation of furfuryl alcohol. For the furfural reactions, the mole fractions of furfural and hydrogen were y_F = 0.010 and y_{H2} = 0.400, respectively. For the furfuryl alcohol reactions, the mole fractions of furfuryl alcohol and hydrogen were y_{FA} = 0.001 and y_{H2} = 0.400, respectively.

Combining results from the reactivity data and CO DRIFTS, a number of general conclusions were reached about the types of sites on which particular reactions occurred. First, because addition of the C18 and the BDT modifiers successively reduced the number of terrace sites available, a systematic reduction in rate may be attributed to a reaction occurring on terrace sites. Additionally, a reaction that has larger site requirements will be affected more strongly by this site reduction. This appeared to be the case for the DC and ADH processes; upon addition of the BDT modifier, the rate of DC was reduced by a factor of ~60, and the rate of ADH was reduced by a factor of ~15. This suggested that the number of contiguous active sites required for the DC process was greater than that necessary for ADH. This hypothesis is consistent with surface science studies of aromatic aldehydes that demonstrated that DC is the dominant process when the molecules can lie flat on the surface.[31] We then hypothesized that ADH occurred from two different structures on the surface—a flat lying structure that occupied a large number of surface sites and that is restricted by the addition of thiol modifiers and an upright structure that occupied fewer sites. Further support for this hypothesis will be discussed in detail below.

The second general conclusion concerns reactions that occur primarily on edges and steps. Because the accessibility to these sites appeared nearly unchanged upon addition of the C18 modifier but was affected by the BDT modifier, cases where reaction rates mimicked this trend were assumed to occur on particle steps and edges. This was the case for the AH and HDO processes. In particular, surface science studies have demonstrated that HDO reactions occur from upright

dx.doi.org/10.1021/cs500598y | ACS Catal. 2014, 4, 3123−3131

structures that do not require large numbers of contiguous surface atoms.[31]

We now focus our attention on ADH and AH. According to the principle of microscopic reversibility, ADH and AH should occur with the same, but reversed, mechanism, since they are reverse processes of each other. Therefore, we would assume that the dependence of these rates on catalyst modification would be the same. This is apparently inconsistent with the data shown in Figure 4 since the rate of ADH was reduced by the C18 modifier (and reduced further by the BDT modifier), suggesting that it occurred from flat-lying structures, while AH was reduced only by the BDT modifier, suggesting that it occurred from upright structures. We explain this discrepancy by noting that the coverage of reactant in these experiments was likely different due to the order of magnitude reduction in mole fraction necessary in order for FA to mimic the amount of FA produced in the experiments performed in generating Figure 2a. Previous surface science work has suggested that adsorbate coverage variations may lead to variations in rates since major shifts in TPD peak position are observed with increasing adsorbate coverage.[22] This coverage effect will be investigated more closely in the discussion of reaction order studies below.

Apparent Activation Energy. In order to probe how site blocking may influence these reaction processes, apparent activation energies for each reaction process were measured and compared to DFT-calculated values on a Pd(111) surface at 1/16 monolayer coverage by Vlachos et al.[20] Reactions were carried out at temperatures ranging from 160 to 190 °C. The results are summarized in Table 1, and the corresponding Arrhenius plots can be found in Figure S7.

Table 1. Apparent Activation Energies for Processes Involved in Scheme 1[a]

catalyst	DC E_a (kJ/mol)	AH E_a (kJ/mol)	ADH E_a (kJ/mol)	HDO E_a (kJ/mol)
5% Pd/Al_2O_3	80 ± 20	50 ± 10	14 ± 7	28 ± 8
C18-5% Pd/Al_2O_3	60 ± 10	13 ± 4	50 ± 20	85 ± 8
BDT-5% Pd/Al_2O_3	70 ± 10	12 ± 5	40 ± 10	82 ± 8
Pd(111)[20]	91.7	77.2	49.2	82.0

[a]DC and AH activation energies were determined using furfural as the reactant; ADH and HDO activation energies were determined using furfuryl alcohol as the reactant. The error reported is the standard error of the slope of the Arrhenius plot using a weighted linear regression. Calculated Pd(111) activation barriers were taken from ref 20.

In general, the apparent activation energies reported in Table 1 may be due to a combination of processes, making exact determination of the limiting process difficult. It is also important to note that all of the calculated barriers were performed with adsorbates in a flat-lying configuration on Pd(111). With these caveats in mind, we can make several observations based on measured values.

First, Table 1 shows that the thiol-coated catalysts have very similar activation barriers for all reaction processes, despite the difference in sulfur coverage. We hypothesize that this similarity is related to the fact that the most abundant surface species for both SAM-coated catalysts is the thiol rather than furfural-derived intermediates, and both thiol-coated catalysts present a relatively dense organic layer at the surface. Further support for this hypothesis is provided by the reaction order studies discussed below. In general, the apparent activation energies for the uncoated catalyst differ substantially, consistent with a much different active site environment.

A possible exception to this difference is for the decarbonylation reaction, which exhibits similar apparent barriers for all catalysts as well as for the prior DFT studies on Pd(111). The apparently similar kinetics among catalysts as well as the agreement with DFT calculations are consistent with a mechanism in which DC requires a relatively large ensemble of sites to proceed through a flat-lying furfural intermediate. In this flat-lying conformation, the aldehyde and furan species inherently occupy nearest neighbor sites and will undergo decarbonylation. Therefore, while increasing thiolate coverage reduces the overall fraction of contiguous sites large enough to permit adsorption of a flat-lying intermediate, once adsorbed in this conformation furfural will undergo decarbonylation via the same mechanism.

Furfural, Furfuryl Alcohol and Hydrogen Reaction Order. Reaction order studies were carried out to investigate how site-blocking from the SAM modifier affects adsorbate coverage. The results are summarized for furfural and furfuryl alcohol as reactants in Table 2. Corresponding power law plots can be found in Figure S9.

In general, a reaction order near unity indicates that the sites required for a particular reaction are not predominantly covered by the reactant, and thus in this range, the rate increases monotonically with increasing partial pressure of the corresponding gas phase molecule. Negative reaction orders indicate that the reaction process is hindered by the presence of that adsorbate. This could be because this reactant is acting as a site blocker for other adsorbates as would be the case in a competitive adsorption model.

In examining Table 2 for reactions involving furfural (DC and AH), several trends become apparent. The reaction order for furfural in DC and AH increased with addition of the SAM modifiers. This effect is attributed to the thiol SAMs preventing significant accumulation of strongly adsorbed furanic intermediates on the terrace sites that are available. On the uncoated

Table 2. Reaction Orders for Processes Depicted in Scheme 1[a]

	furfural R.O.		hydrogen R.O.		furfuryl alcohol R.O.		hydrogen R.O.	
catalyst	DC	AH	DC	AH	ADH	HDO	ADH	HDO
5% Pd/Al_2O_3	0.3(2)	0.5(2)	−0.5(3)	0.3(4)	1.1(1)	1.0(2)	−0.03(7)	0.10(5)
C18-5% Pd/Al_2O_3	0.85(6)	0.80(1)	−0.36(9)	0.54(8)	1.12(2)	0.96(8)	0.32(6)	0.24(7)
BDT-5% Pd/Al_2O_3	0.7(2)	0.79(2)	−0.3(2)	0.76(6)	0.9(2)	0.90(6)	0.2(1)	0.32(6)

[a]Reaction order experiments for DC and AH were performed with furfural; experiments for ADH and HDO were performed with furfuryl alcohol. The numbers in parentheses represent the uncertainty in the least significant digit. The uncertainty is the standard error of the slope of the power law plot using a weighted linear regression.

dx.doi.org/10.1021/cs500598y | ACS Catal. 2014, 4, 3123−3131

surface, the somewhat lower order is attributed to the fact that furfural adsorbs strongly on the surface, which limits the available active sites. The higher order for the coated catalysts suggests that the available sites for DC and (to a lesser degree) AH bind furfural more weakly, suppressing its surface accumulation. The reaction order for hydrogen in DC was negative in all cases, consistent with the fact that hydrogen was not involved in the DC process. Hydrogen may have acted as a site blocker for furfural in this case, reducing the coverage of furfural on the surface. Additionally, the hydrogen reaction order for AH increased on the thiol-coated catalysts, indicating that hydrogen coverage was also reduced when the SAMs were present, similar to furfural.

The reaction order for furfuryl alcohol in ADH and HDO, Table 2, was near unity on both the uncoated and thiol-coated catalysts. This is consistent with the fact that the concentration of furfuryl alcohol in these reactions was an order of magnitude smaller than furfural to mimic the low concentration of furfuryl alcohol produced under the furfural hydrogenation reaction conditions, and so the surface coverage of furfuryl alcohol was likely small on all catalysts. Correspondingly, the reaction order for hydrogen in HDO was near zero in all cases, indicating that additional hydrogen did not significantly assist the reaction rate because there was enough surface hydrogen available. The hydrogen reaction order increased slightly on the thiol-coated catalysts, consistent with the idea that coverage of all species was reduced by the presence of the SAM.

The reaction order in hydrogen for the ADH reaction presents an interesting trend. One would expect, since the reaction requires no stoichiometric hydrogen, that the reaction order would be negative in all cases since hydrogen would act as a site blocker. However, the reaction order actually switched from near zero to slightly positive on the thiol-coated catalysts. This could be due to the effect of hydrogen lowering the concentration of strongly bound flat-lying intermediates on the surface or with the existence of a reaction pathway for ADH that involves dehydrogenation of furfuryl alcohol to the acyl species before addition of a single hydrogen atom to form the aldehyde.[20]

DISCUSSION

From the results presented here, the following interpretations were made regarding the effect of thiolate modifiers on the furfural reaction network.

1) The decarbonylation reaction mechanism appeared to be similar on modified and unmodified catalysts. From comparisons between reactivity and site availability, the rate of DC was systematically reduced with increasing coverage of surface sulfur, consistent with the hypothesis that furfural needed a larger ensemble of contiguous active sites to bind in the multicoordinated adsorption geometry required for DC. Apparent activation energies were found to be nearly the same for this process on all catalysts tested, and the DC reaction order increased upon addition of thiol modifiers. This suggested that the coverage of strongly bound furanic species on terrace sites was reduced due to a change in average adsorption energy; on coated catalysts, the available sites for DC bound furfural more weakly, leading to a higher reaction order. Though this effect cannot be definitively resolved without direct measurement of adsorption equilibrium constants, the data suggest that the thiols present a fairly simple perturbation to the mechanism without altering the rate-limiting step.

2) Comparison between site availability and reactivity provided insight with respect to the sites required for the remaining processes: aldehyde hydrogenation/alcohol dehydrogenation and hydrodeoxygenation. Previous surface science studies showed that high coverage of these aromatic oxygenates can cause the flat-lying and upright structures to coexist,[31] suggesting that AH and ADH reactions could proceed through either type of intermediate. Under furfuryl alcohol hydrogenation conditions, the application of thiol coatings decreased the ADH rate by a much smaller factor than the DC rate, consistent with the participation of intermediates with reduced site requirements in ADH. Under furfural hydrogenation conditions where surface crowding is more severe, the addition of thiols has even less of an effect on the AH rate. Hypothetically this is due to a low coverage of more flat-lying AH/ADH intermediates even on the uncoated catalyst. As discussed above, comparison between reactivity and site availability suggests that HDO occurred primarily on particle edges and steps from an upright structure of furfuryl alcohol. Even in the presence of high sulfur coverage, the production of methylfuran was unaffected by the presence of the C18-modifier and modestly reduced by the BDT-modifier. Thus, whereas DC preferentially occurs on terraces and HDO on step edges, AH/ADH has intermediate site requirements, and the dominant pathway may be dictated by reaction conditions.

While reactivity/structure relationships suggest that AH and ADH occurred on both terrace and edge sites and that HDO occurred primarily on particle edges, comparison between apparent activation energies on the coated and uncoated catalysts provided evidence that the presence of the modifiers affected the rate limiting mechanisms for these processes. This effect may be, in part, related to the role of hydrogen since the presence of sulfur has been shown to hinder both hydrogen adsorption and diffusion on single crystal surfaces.[32,33]

3) The mechanism by which the modifiers improved selectivity toward the hydrogenation pathways was the same for the thiol-coated catalysts. In other words, the improved selectivity behavior observed using the denser BDT-modified catalyst was fundamentally the same as the C18 catalyst, but the higher sulfur coverage essentially made this coating more effective for restricting the undesired DC process. Apparent activation energies were found to be statistically identical for all reaction processes between the BDT and C18 catalysts. This similarity likely results from the fact that both SAMs serve to isolate Pd sites, creating a more uniform reaction environment than on the uncoated surface.

In order to quantitatively determine the effect of thiol coverage on the specific kinetic properties for this reaction network (e.g., inherent rate constants and adsorption equilibrium constants), we developed a Langmuir–Hinshelwood kinetic model that is included in the Supporting Information. A primary conclusion from the modeling results is that the dense BDT coating is associated with elementary step reaction rates that are far higher than would be predicted on the basis of CO chemisorption. This result is reflected in the data reported above, where (for example) a relatively high rate for HDO is achieved (Figure 2), even though site availability is drastically reduced compared to the uncoated and C18 coated catalysts. While the HDO reactivity qualitatively trends with edge site availability, the lack of exact correlation between edge site availabilities and HDO rates indicates that CO DRIFTS likely is not a sensitive probe for all active sites for the reaction

dx.doi.org/10.1021/cs500598y | ACS Catal. 2014, 4, 3123−3131

and that a more thorough description of such sites may be valuable for catalyst design.

Scheme 2 summarizes the reactions that occurred on uncoated and thiol-coated Pd catalysts based on site availability,

Scheme 2. Proposed Reaction Pathways for Furfural and Furfuryl Alcohol on Uncoated and Thiol-Coated Catalysts

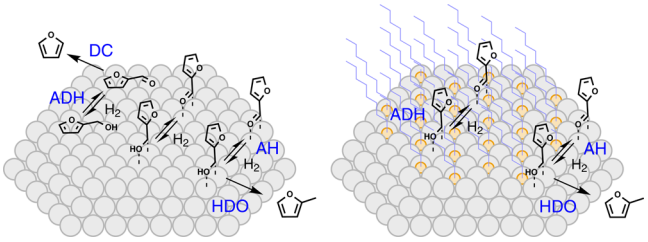

apparent activation energies, and reaction orders. On the uncoated catalyst, furfural and furfuryl alcohol adsorbed in either a flat-lying or an upright conformation. These two adsorbates hydrogenated/dehydrogenated in both configurations. However, decarbonylation required that adsorbates adopt the flat-lying conformation, while hydrodeoxygenation occurred from an upright conformation. On the thiol-coated catalysts, the adsorbates tended to adopt the upright conformation, leading to drastically decreased rate of decarbonylation. This kind of orientation-selectivity effect for decarbonylation and hydrodeoxygenation has also been seen in surface science studies.[31]

On uncoated catalysts, the reactants adsorbed in a flat-lying conformation on terraces or in an upright conformation on both terraces and edges; reactants were restricted to the upright conformation on both terraces and edges when the thiol coating was present.

CONCLUSIONS

Here, we report results for a comprehensive kinetic investigation on the effect of increasing SAM-modifier concentration during furfural hydrogenation on uncoated, 1-octadecanethiol, and benzene-1,2-dithiol coated Pd/Al_2O_3 heterogeneous catalysts. Addition of C18 and BDT surface modifiers systematically increased the hydrogenation selectivity of furfural to furfuryl alcohol and methylfuran. Ambient-pressure XPS experiments demonstrated that the metal−sulfur bonds were not appreciably changed over the course of the reaction, implying that the thiolate monolayer was stable under reaction conditions. Decarbonylation was found to occur on particle terrace sites via similar mechanisms on both coated and uncoated catalysts. Aldehyde hydrogenation and the reverse process alcohol dehydrogenation occurred on particle terraces and steps via reaction of both flat-lying and upright furfural, with reaction from the upright structure being more important. Hydrodeoxygenation occurred primarily at particle edges and steps likely from an upright conformation of furfuryl alcohol. The rate of this reaction was hardly decreased by increasing sulfur coverage. The mechanism by which the BDT- and C18-modifiers enhance selectivity toward hydrogenation products was thus the same; improved selectivity with the BDT modifier was attributed to the higher sulfur coverage which was more effective for restricting the undesired decarbonylation process. Increasing thiol density on the surface resulted in a decrease in coverage of strongly bound species, as evidenced by reduction in available sites in CO DRIFTS and increase in reaction order with SAM modification. Thus, SAM modification can serve the role of isolating certain types of surface sites; intriguingly, the isolated sites are highly active for hydrodeoxygenation while being much less reactive toward undesired decarbonylation.

ASSOCIATED CONTENT

Supporting Information

Figures as described in the text. Section regarding the Langmuir−Hinshelwood model considered in the discussion. This material is available free of charge via the Internet at http://pubs.acs.org.

AUTHOR INFORMATION

Corresponding Author

*E-mail: will.medlin@colorado.edu.

Author Contributions

†These authors (S.H.P. and C.A.S.) contributed equally.

Notes

The authors declare no competing financial interest.

ACKNOWLEDGMENTS

C.A.S. acknowledges partial support from a graduate fellowship from ConocoPhillips/Phillips66. S.H.P. acknowledges the Colorado Center for Biorefining and Biofuels Fellowship Grant and the Engineering Excellence Fund of the University of Colorado. We thank April Corpuz for her assistance running the reaction order experiments. We also thank Samuel Tenney and Peter Sutter at Brookhaven National Laboratory Center for Functional Nanomaterials for beamtime at the National Synchrotron Light Source, beamline X1A1, and assistance performing ambient-pressure XPS experiments. C.A.S. would like to thank Prof. D. E. Clough for helpful discussions regarding multivariate statistics and modeling. The work was supported by the US Department of Energy, Office of Science, Basic Energy Sciences Program, Chemical Sciences, Geosciences and Biosciences Division (DE-FG02-10ER16206), and the US National Science Foundation (CHE-1149752).

REFERENCES

(1) Schoenbaum, C. A.; Schwartz, D. K.; Medlin, J. W. *Acc. Chem. Res.* **2014**, *47*, 1438−1445.
(2) Love, J. C.; Wolfe, D. B.; Haasch, R.; Chabinyc, M. L.; Paul, K. E.; Whitesides, G. E.; Nuzzo, R. E. *J. Am. Chem. Soc.* **2003**, *125*, 2597−2609.
(3) Marshall, S. T.; O'Brien, M.; Oetter, B.; Corpuz, A.; Richards, R. M.; Schwartz, D. K.; Medlin, J. W. *Nat. Mater.* **2010**, *9*, 853−858.
(4) Marshall, S. T.; Schwartz, D. K.; Medlin, J. W. *Langmuir* **2011**, *27*, 6731−6737.
(5) Makosch, M.; Lin, W.; Bumbálek, V.; Sá, J.; Medlin, J. W.; Hungerbühler, K.; van Bokhoven, J. A. *ACS Catal.* **2012**, *2*, 2079−2081.
(6) Kahsar, K. R.; Schwartz, D. K.; Medlin, J. W. *ACS Catal.* **2013**, *3*, 2041−2044.
(7) Wu, B.; Huang, H.; Yang, J.; Zheng, N.; Fu, G. *Angew. Chem., Int. Ed.* **2012**, *51*, 3440−3443.
(8) Gopidas, K. R.; Whitesell, J. K.; Fox, M. A. *Nano Lett.* **2003**, *3*, 1757−1760.
(9) Lu, C.; Chang, F. *ACS Catal.* **2011**, *1*, 481−488.
(10) Lu, F.; Ruiz, J.; Astruc, D. *Tetrahedron Lett.* **2004**, *45*, 9443−9945.
(11) Cargnello, M.; Wieder, N. L.; Canton, P.; Montini, T.; Giambastiani, G.; Benedetti, A.; Gorte, R. J.; Fornasiero, P. *Chem. Mater.* **2011**, *23*, 3961−3969.

(12) Kim, J.-H.; Park, J.-S.; Chung, H.-W.; Boote, B. W.; Lee, T. R. *RSC Adv.* **2012**, *2*, 3968−3977.
(13) Moreno, M.; Kissell, L. N.; Jasinski, J. B.; Zamborini, F. P. *ACS Catal.* **2012**, *2*, 2602−2613.
(14) Alvarez, J.; Liu, J.; Román, E.; Kaifer, A. E. *Chem. Commun.* **2000**, 1151−1152.
(15) Nørskov, J. K.; Bligaard, T.; Hvolbæk, B.; Abild-Pedersen, F.; Chorkendorff, I.; Christensen, C. H. *Chem. Soc. Rev.* **2008**, *37*, 2163−2171.
(16) Bond, G. C. *Platinum Met. Rev.* **1975**, *19*, 126−134.
(17) Zhang, H.; Jin, M.; Xiong, Y.; Lim, B.; Xia, Y. *Acc. Chem. Res.* **2013**, *46*, 1783−1794.
(18) Serrano-Ruiz, J. C.; West, R. M.; Dumesic, J. A. *Annu. Rev. Chem. Biomol. Eng.* **2010**, *1*, 79−100.
(19) Sitthisa, S.; Resasco, D. E. *Catal. Lett.* **2011**, *141*, 784−791.
(20) Vorotnikov, V.; Mpourmpakis, G.; Vlachos, D. G. *ACS Catal.* **2012**, *2*, 2496−2504.
(21) Pang, S. H.; Medlin, J. W. *ACS Catal.* **2011**, *1*, 1272−1283.
(22) Pang, S. H.; Schoenbaum, C. A.; Schwartz, D. K.; Medlin, J. W. *Nat. Commun.* **2013**, *4*, 2448.
(23) Yang, Y.-C.; Lee, Y.-L.; Yang, L.-Y. O.; Yau, S.-L. *Langmuir* **2006**, *22*, 5189−5195.
(24) Porter, M. D.; Bright, T. B.; Allara, D. L.; Chidsey, C. E. D. *J. Am. Chem. Soc.* **1987**, *109*, 3559−3568.
(25) Kalinin, S. V. *Adv. Funct. Mater.* **2013**, *23*, 2468−2476.
(26) Shirley, D. *Phys. Rev. B* **1972**, *5*, 4709−4714.
(27) Bain, C. D.; Biebuyck, H. A.; Whitesides, G. M. *Langmuir* **1989**, *5*, 723−272.
(28) Castner, D. G.; Hinds, K.; Grainger, D. W. *Langmuir* **1996**, *12*, 5083−5086.
(29) Laibinis, P. E.; Bain, C. D.; Whitesides, G. M. *J. Phys. Chem.* **1991**, *95*, 7017−7021.
(30) Schoenbaum, C. A.; Schwartz, D. K.; Medlin, J. W. *J. Catal.* **2013**, *303*, 92−99.
(31) Pang, S. H.; Román, A. M.; Medlin, J. W. *J. Phys. Chem. C* **2012**, *116*, 13654−13660.
(32) Gravil, P. A.; Toulhoat, H. *Surf. Sci.* **1999**, *430*, 176−191.
(33) Wilke, S.; Scheffler, M. *Surf. Sci.* **1995**, *329*, L605−L610.